frontiers in Marine Science

ORIGINAL RESEARCH
published: 29 October 2018
doi: 10.3389/fmars.2018.00387

Symbiont Chloroplasts Remain Active During Bleaching-Like Response Induced by Thermal Stress in *Collozoum pelagicum* (Collodaria, Retaria)

Emilie Villar[1], Vincent Dani[2], Estelle Bigeard[1], Tatiana Linhart[1], Miguel Mendez-Sandin[1], Charles Bachy[1], Christophe Six[1], Fabien Lombard[3], Cécile Sabourault[2] and Fabrice Not[1]**

[1] Sorbonne Université, CNRS – UMR7144 – Ecology of Marine Plankton Group – Station Biologique de Roscoff, Roscoff, France, [2] Université Côte d'Azur, Institut de Biologie Valrose UMR7277, Nice, France, [3] Sorbonne Université, CNRS – UMR 7093, Laboratoire d'Océanographie de Villefranche (LOV), Observatoire Océanologique, Villefranche-sur-Mer, France

OPEN ACCESS

Edited by:
Matthew D. Johnson, Woods Hole Oceanographic Institution, United States

Reviewed by:
Anthony William Larkum, University of Technology Sydney, Australia
Manuel F. G. Weinkauf, Université de Genève, Switzerland

***Correspondence:**
Emilie Villar
emilie.villar1@gmail.com
Fabrice Not
not@sb-roscoff.fr

Specialty section:
This article was submitted to Marine Ecosystem Ecology, a section of the journal Frontiers in Marine Science

Received: *08 June 2018*
Accepted: *03 October 2018*
Published: *29 October 2018*

Citation:
Villar E, Dani V, Bigeard E, Linhart T, Mendez-Sandin M, Bachy C, Six C, Lombard F, Sabourault C and Not F (2018) Symbiont Chloroplasts Remain Active During Bleaching-Like Response Induced by Thermal Stress in Collozoum pelagicum (Collodaria, Retaria). Front. Mar. Sci. 5:387. doi: 10.3389/fmars.2018.00387

Collodaria (Retaria) are important contributors to planktonic communities and biogeochemical processes (e.g., the biologic pump) in oligotrophic oceans. Similarly to corals, Collodaria live in symbiosis with dinoflagellate algae, a relationship that is thought to explain partly their ecological success. In the context of global change, the robustness of the symbiotic interaction, and potential subsequent bleaching events are of primary interest for oceanic ecosystems functioning. In the present study, we compared the ultrastructure, morphology, symbiont density, photosynthetic capacities and respiration rates of colonial Collodaria exposed to a range of temperatures corresponding to natural conditions (21°C), moderate (25°C), and high (28°C) thermal stress. We showed that symbiont density immediately decreased when temperature rose to 25°C, while the overall Collodaria holobiont metabolic activity increased. When temperature reached 28°C, the holobiont respiration nearly stopped and the host morphological structure was largely damaged, as if the host tolerance threshold has been crossed. Over the course of the experiment, the photosynthetic capacities of remaining algal symbionts were stable, chloroplasts being the last degraded organelles in the microalgae. These results contribute to a better characterization and understanding of temperature-induced bleaching processes in planktonic photosymbioses.

Keywords: heat stress, photosymbiosis, bleaching, dinoflagellate, Collodaria, Radiolaria, Retaria, plankton

INTRODUCTION

Retaria encompass Foraminifera and Radiolaria *sensu stricto* or Radiozoa. Within Radiozoa, Collodaria have been recently unraveled as key players in oceanic ecosystems (Biard et al., 2016; Guidi et al., 2016). Previously overlooked because of their fragility, the use of non-destructive, *in situ*, imaging tools showed that Collodaria represents nearly 30% of zooplankton biomass at subsurface in oligotrophic oceans (Biard et al., 2016). Collodaria were also reported as central actors in plankton community networks related to carbon export to the deep ocean via both primary

production and vertical flux (Guidi et al., 2016). Initially described by E. Haeckel toward the end of the 19th century (Haeckel, 1887), Collodaria have been little studied so far, with only a few landmark studies conducted on radiolarian morphology and physiology (Anderson, 1983).

Collodaria are unicellular organisms that live either solitary (cell size ∼1 mm) or form colonies up to a few centimeters long. Each colony is composed of hundreds to thousands of cells agglomerated in a gelatinous matrix. All cells, individually represented by a spherical structure called the central capsule, are connected together through cytoplasmic extensions and some particular species can bear a siliceous skeleton (Anderson, 1976a,b). Collodaria feed on prey from the surrounding environment but can be considered as mixotrophic organisms, since they also rely on symbiotic interactions with photosynthetic dinoflagellates. Swanberg (1983) suggested that photosymbiosis provides Retaria with the minimum energy to subsist, while their energy and nutrients for growth would come from their heterotrophic regime. Collodaria can consume 4% of their symbionts everyday (Anderson, 1983) and a part of the photosynthates are transferred to the host, mostly as lipid storage pool (Anderson et al., 1983). Microalgae symbionts isolated from the collodarian species *Collozoum* spp. have been recently identified as *Brandtodinium nutricula*, a dinoflagellate species belonging to the Peridiniales order (Probert et al., 2014). As *B. nutricula* can be cultivated in host-free media and has been found in association with different radiolarian hosts and even with the jellyfish *Velella velella*, this microalga is thought to be a generalistic symbiont having free-living stages (Decelle et al., 2015).

The breakdown of the symbiotic associations in corals, so-called coral bleaching, has been originally described by Glynn (1984), who depicted coral bleaching as a reaction to environmental constraints, due to the massive loss of symbiotic algae, or alternatively as a decline of their photosynthetic pigment content. Recent projections suggest that more than half of the coral reefs worldwide will experience several bleaching events by the year 2100, as a consequence of ocean temperature rise of 1–1.8°C (Logan et al., 2014). Coral bleaching has significant deleterious consequences on coral reef ecosystem functioning and as a result, on several countries economy and food supply (Hoegh-Guldberg et al., 2007). Numerous studies have tried to decipher the relationships between corals -or other cnidarians such as sea anemones- and their symbionts upon environmental perturbations. Although bleaching events involve the whole holobiont and all possible interactions between its biotic components (Baird et al., 2009), in cnidarians most studies considered bleaching as being induced by the microalgal partner release (reviewed in Lesser, 2011). One of the proposed mechanisms suggests the production of reactive oxygen species (ROS) when symbiont photosynthesis is impaired by heat stress (Lesser, 2006). These ROS lead to the death of the host cells by triggering apoptosis, notably through the induction of protease enzymes (Cikala et al., 1999). During the stress and death of the host cells, microalgal symbiotic cells can be either healthy (Baghdasarian and Muscatine, 2000) or damaged (Fujise et al., 2014). In the later case, it is unclear whether the symbiont damages are due to the host cell apoptosis or to other symbiont related processes, such as programmed cell death (PCD) or host autophagic digestion (Dunn et al., 2007; Paxton et al., 2013).

Considering the potential impact of bleaching in Collodaria on the marine ecosystem functioning and the lack of recent studies on their biology, this study aims at a better characterization of their functional behavior. We performed a controlled thermal stress experiment on Collodaria to investigate potential plankton bleaching and the photosymbiosis response to elevated temperatures using both morphological and physiological analyses.

MATERIALS AND METHODS

Experimental Design

Collodarian colonies were collected in the bay of Villefranche-sur-Mer (France, 43°41′10″ N, 7°18′50″ E) using a Regent plankton net (680 μm mesh size) handheld from a boat, immediately handpicked and transferred into clean beakers filled with seawater filtered over 0.2 μm filters. Colonies were incubated at ambient seawater temperature (21°C) for 3–4 h to allow self-cleaning of particles embedded in their gelatinous matrix. A total of 300 colonies with similar morphotypes were transferred individually into two 17L-Kreisel tank aquaria (JHT-17G, Exotic Aquaculture, Hong-Kong) filled with 0.2 μm filtered seawater and placed in two distinct thermostatic incubators set at 21°C (TC135S, Lovibond Water testing, United Kingdom). As treatments were performed in single experimental units (called pseudoreplication by Hurlbert, 1984), colonies were randomly placed in the two aquaria. Two liters of 0.2 μm filtered seawater from the Kreisel tanks were changed on a daily basis. Electroluminescent diode ramps (Easyled 6800 K°, Aquatlantis, Portugal) provided constant white light at 100 μmol photon m^{-2} s^{-1}. Colonies were further exposed to two thermal treatments during 3 days (T0, T1, and T2). In one aquarium, the control treatment (CT) remained at 21°C over the course of the experiment. In the other aquarium, the temperature of the stressed treatment (ST) was raised from 21°C (T0), to 25°C (T1) on the first day and then from 25°C to 28°C (T2) on the second day. The water temperature increased by 1°C per hour sufficiently in advance to enable a 12 h-acclimation before sampling. In the following text, a "condition" refers to the unique combination of a treatment and a sampling time point (e.g., CT-T0).

Phylogenetic Analysis

18S ribosomal DNA gene sequences from the Collodarian host and the dinoflagellate symbionts of 30 holobiont specimens collected during the experiment were retrieved from the transcriptome data (see details in **Supplementary Text 1**). Briefly, for each sample, host and symbiont sequences were aligned separately with reference sequences using MAFFT (Katoh et al., 2002). Phylogenetic trees were obtained using maximum likelihood reconstruction method in RAxML (Stamatakis, 2014), allowing the genetic identification of the host and the symbiont species.

Transmission Electron Microscopy (TEM)

For each condition, Collodarian specimens were collected in triplicates and independently fixed for 2 h at room temperature with 2.5% glutaraldehyde in a mix of cacodylate buffer (0.1 M, pH 7.4)/artificial seawater, then washed with 0.1 M cacodylate buffer (pH 7.4) and postfixed with 1% osmium tetroxide in cacodylate buffer containing 1% potassium ferrocyanide. Each samples were embedded in Epon resin after 10 min dehydration in 90% acetone and 2 baths of 10 min in acetone 100%. Ultrathin sections (70–80 nm) of colony parts were obtained using a diamond knife mounted on an ultramicrotome (Ultracut S, Leica) and placed on copper TEM grids coated with formvar film. To increase the contrast, the grids were treated with conventional uranyl acetate stain followed by lead citrate. Samples were observed under a JEOL JEM 1400 transmission electron microscope equipped with a CCD camera (Morada, Olympus SIS).

Oxygen Measurements

Oxygen consumption was measured using oxygen optodes, as described in Lilley et al. (2014). Each sample was made of two colonies incubated together in 5 mL tubes filled with filtered seawater and equipped with light-sensitive oxygen spots (PreSens Precision Sensing GmbH, Germany). For each condition, 6 measurements were made: 5 replicates and an additional control tube filled with 0.2 μm filtered seawater only that was used for blank corrections. This control tube therefore records the background respiration of the few organisms still present since neither 0.2 μm filtered seawater nor containers were sterile. After 30 min of dark-acclimation, oxygen was measured using a Fibox 3 optical oxygen meter (PreSens) every 20 min during 2 h. Light (100 μmol photon m^{-2} s^{-1}) was then switched on for 2 h and oxygen was measured again every 20 min for 2 h under light exposure.

After calibration, the phase delay measured by the sensor was converted into O_2 concentration (in μmol L^{-1}). Linear regressions between oxygen concentration against time were fitted through all data points for each replicate and for dark and light measurements separately. Values showing standardized residues <-1.5 and >1.5 were considered as outliers and removed from the dataset to ensure linearity (54 out of 384 measures). Slopes of the fitted regression gave individual consumption rates (μmol O_2 $L^{-1}h^{-1}$) and blank slopes were removed from experimental slopes to remove the water background respiration associated with the use of non–sterile water/containers [see Lilley et al. (2014)]. In all cases, this background O_2 change was negligible (average slope: 0.08) compared to the respiration/photosynthesis signal recorded (average slope: 0.21). Respiration rates were estimated as the slope during the dark experiment and gross photosynthesis rates were computed as differences of slopes between light (net photosynthesis) and dark. The respiration/photosynthesis signal recorded corresponds then to the net respiration and photosynthesis of the holobiont (including host, symbionts, and the associated microbiota). For normalization, rates were divided by the colony biomass estimated from binocular inspection (see the following morphological measurement methods). The Q_{10} temperature coefficient is the factor by which the reaction rate increases when the temperature is raised by ten degrees. It has been calculated using the following equation: $Q_{10} = \left(\frac{R_2}{R_1}\right)^{\left(\frac{10}{T_2-T_1}\right)}$ where R_1 and R_2 are the reaction rates at the corresponding temperatures T_1 and T_2.

Chlorophyll Fluorescence Measurements Coupled With Microscopy

For each condition, 5 collodarian colonies were transferred to cavity slides and maintained with a coverslip to prevent them from moving. For every 5 replicated colonies, photosynthetic parameters of individual symbiotic microalgae were measured on three different fields of observation using a Pulse Amplitude Modulated fluorometer coupled to a microscope (MICROSCOPY-PAM; Walz, Effeltrich, Germany), equipped with a 10 × objective lens. After the colonies were incubated in the dark for at least 5 min, the basal level of fluorescence (F_0) was measured under modulated light (9 μmol photons m^{-2} s^{-1}, frequency: 8 Hz at 625 nm), and a saturating light pulse (1707 μmol photons m^{-2} s^{-1}, during 8 × 60 ms at 625 nm) allowed determining the maximum fluorescence level (F_M). The Dark-adapted maximal quantum Yield (F_V/F_M) of photosystem II (PSII) was computed as follows:

$$F_V/F_M = (F_M - F_0)/F_M$$

The colonies were then exposed to actinic light (463 μmol photons m^{-2} s^{-1} at 625 nm) during 2 min followed by another saturating light pulse to measure the light-adapted PSII fluorescence yield (F_V'/F_M'; Genty et al., 1989). Pilot experiments and light curves were previously performed to determine the optimal duration of the dark incubation and actinic light intensity. The saturating pulse settings were adjusted according to preliminary experiments performed on cultures of *B. nutricula* (**Supplementary Text 2**).

For every colony, a number of 6 to 15 areas of interest, corresponding to single symbiotic cells, were selected on each picture (see **Supplementary Figure S1**). Outliers were removed when measured values were inconsistent (e.g., $F_V/F_M = 0$ or 1), being mostly due to field depth impairments. Overall, we obtained between 13 and 45 measurements for each of the 5 replicate colonies per experimental condition. To avoid bias due to these sampling size differences between conditions to compare, the F_V/F_M medians were computed for each microscopic field (3 microscopic fields per colony; 5 replicated colonies per condition).

Morphological Measurements

Images of all colonies used for oxygen and PAM fluorescence analyses were acquired under a binocular microscope (Zeiss Stemi SV11 mounted with an Olympus DP21 camera system) and analyzed using the ImageJ software (Rasband, 1997)[1]. Stressed colonies at sampling time 2 (ST-T2) were too degraded to be manipulated and observed under binocular microscope. For this

[1]https://imagej.nih.gov/ij/

specific condition, morphological measurements were performed for one colony and data are provided as indicative trends, while 13 to 17 replicates were accounted for other conditions. Correction factors were applied to normalize measurements in function of the different magnifications used to take each picture. On large field of view, we used image thresholding of ImageJ to measure full colonies area, width and we derived biovolume estimates from the prolate ellipsoid equation described in Biard et al. (2016). We also enumerated the total number of central capsules present on the observable part of the colonies using the automated cell count functionality of ImageJ. On zoomed in fields of view, we measured each central capsule area along with central capsule area covered by microalgal symbionts. As previously, we counted the total number of central capsules on the observable part of the colonies. We also enumerated the symbionts observed between central capsules (i.e., in the matrix) and measured their areas. At this magnification the symbiont cell area was homogeneous, we derived the number of symbionts per central capsule by dividing their total area by the average area of a symbiont ($3x10^{-4}mm^2$). Symbiont density was thus expressed as the number of symbionts per area. Carbon content was derived from the central capsule counts using a conversion factor of 131 ng C per capsule (Michaels et al., 1995).

Statistical Analysis

All the statistical analysis and associated figures were performed using R version 3.5.1 (R Core Team, 2013). For fluorescence and oxygen analyses, pairwise permutation tests from the rcompanion library have been used to test for significance of the interaction treatment-sampling time effect.

For symbiont density analysis, a *t*-test was applied to compare the regression slopes at each sampling time between the two treatments.

RESULTS

Colonies were identified as *Collozoum pelagicum* by phylogenetic analysis of the 18S rDNA gene sequences (NCBI accession MG907123, **Supplementary Figure S2**) onto a reference tree published in Biard et al. (2015). We were also able to retrieve 18S rDNA sequences of a dinoflagellate identified as *B. nutricula* by phylogenetic placement (NCBI accession MG905637, **Supplementary Figure S3**), confirming that *C. pelagicum* hosts *B. nutricula* as symbiotic algae.

C. pelagicum Morphological Changes Upon Heat Stress

Depending on colony size, an average of 800 (*SD* = 300) *C. pelagicum* cells were agglomerated in the gelatinous matrix, corresponding to an average density of 10 cells per mm^2 of colony surface. (**Table 1** and **Supplementary Table S1**). Cells were distributed in the matrix forming defined compartments (**Figure 1a**). Central capsules, appearing bright under the microscope (**Figure 1a**), exhibited a size ranging from 100 to 150 μm. Each central capsule contained a large electron dense droplet, an endoplasm and an ectoplasm (**Figure 1b**). Sudan Black staining suggested that this droplet, surrounded by a vacuolar membrane was constituted of fibrous elements and lipids. The endoplasm contained multiple nuclei displaying fibrillar nucleoplasm chord-like structures of chromatin attached to the inner surface of the nuclear membrane (**Figures 1c,d**). The endoplasm was delimited from the ectoplasm by a multiple layer membrane (**Figure 1e**).

Brandtodinium nutricula cells were always within cytoplasmic structures, either spread in the gelatinous matrix or closely associated to the central capsules (**Figures 1a,b**) and exhibited a thick cell wall and no flagella. *B. nutricula* were enclosed in a vacuole and separated from the *C. pelagicum* ectoplasm by a vacuolar membrane (**Figure 1f**). *B. nutricula* cells contained pyrenoid-bearing lobed chloroplasts, located essentially at the cell periphery, and associated with starch granules. Comparisons of phenotypes from control colonies (CT at 21°C) to heat stressed colonies (ST) at 3 sampling times (T0:21°C, T1:25°C, and T2:28°C) demonstrated that the general morphology of control colonies was preserved during the entire experiment. The polysaccharide matrix surrounded the evenly distributed central capsules and the compartments forming the colony remained visible (**Figures 2a,b**). In heat-stressed conditions, the central capsules from the colonies were still observable but irregularly distributed (**Figures 2c,d**). The gelatinous matrix was altered at 25°C and completely disorganized at 28°C, while colony compartments disappeared, being replaced by large bubbles inside the colonies (**Figure 2d**). With respect to ultrastructural features, ectoplasms were degraded, revealing large spaces around vacuoles, at T2 for CT colonies (**Figures 2e,f**) and earlier (from T1) in ST colonies (**Figure 2g**). Ectoplasm of ST-T2 colonies completely shrunk (**Figure 2h**). Compared to freshly collected specimens, both control and thermal stress experiments showed highly condensed chromatin in their nuclei, with an increase in electron-dense filaments (**Figures 1c,d**, **2i–l**).

Physiological Impact of Heat Stress on *C. pelagicum*

At seawater temperature, the respiration rate was of 3.94 (*SD* = 0.99) $\mu LO_2\ mgC^{-1}\ h^{-1}$ (**Table 1**, **Figure 3**, and **Supplementary Tables S1, S2**). The incubation conditions did not affect significantly the respiration rates in control colonies, with values of 4.58 (*SD* = 0.83) $\mu LO_2\ mgC^{-1}\ h^{-1}$ at T1 and 4.84 (*SD* = 1.25) $\mu LO_2\ ind^{-1}\ h^{-1}$ at T2. For heat-stressed colonies, the respiration rates slightly increased at 25°C, reaching 5.82 (*SD* = 1.62) $\mu LO_2\ mgC^{-1}\ h^{-1}$, and decreased markedly to 2.94 (*SD* = 1.56) $\mu LO_2\ mgC^{-1}\ h^{-1}$ at 28°C.

The experimental conditions induced a decrease of the average *B. nutricula* cell density, from nearly 80 symbionts mm^{-2} at T0 and T1, down to 59 symbionts mm^{-2} at T2, for control colonies (**Table 1** and **Figure 4**). The symbiont density decrease occurred significantly faster in heat-stress conditions with as few as 60 symbionts mm^{-2} at T1 (25°C) already. The regression line slopes between T0 and T1 were significantly different with a stronger drop in symbiont densities in stressed colonies compared to controls (*p*-value = 0.05). At T2 (28°C), symbiont density kept decreasing down to 50 symbionts mm^{-2}, but the reaction norm

TABLE 1 | Summary of the statistics of the morphological and physiological measurements in control (CT) and heat-stressed (ST) colonies of *Collozoum pelagicum* at 3 sampling times (T0, T1, and T2).

Sampling time	Treatment	Central capsule density (nb/mm$_2$)	Central capsule average size (mm$_2$)	Holobiont biovolume (mm^3)	Symbiont density (nb/mm$_2$)	Respiration rate (µl O2.mgC-1.h-1)	Photosynthesis rate (µl O2.mgC-1.h-1)	Fv/Fm
T0	CT	9 ± 2 (*n* = 16)	0.017 ± 0.004 (*n* = 16)	135 ± 49 (*n* = 16)	74 ± 17 (*n* = 16)	3,9 ± 1 (*n* = 4)	4,4 ± 2 (*n* = 4)	0.569 ± 0.021 (*n* = 6)
T1	CT	10 ± 1 (*n* = 13)	0.018 ± 0.004 (*n* = 13)	164 ± 38 (*n* = 13)	81 ± 20 (*n* = 13)	4,6 ± 0,8 (*n* = 5)	4,2 ± 0,7 (*n* = 5)	0.578 ± 0.017 (*n* = 5)
T1	ST	10 ± 1 (*n* = 14)	0.016 ± 0.004 (*n* = 14)	120 ± 57 (*n* = 15)	60 ± 9 (*n* = 14)	4,8 ± 1,3 (*n* = 4)	3,3 ± 1,3 (*n* = 4)	0.603 ± 0.04 (*n* = 5)
T2	CT	12 ± 3 (*n* = 15)	0.015 ± 0.003 (*n* = 15)	159 ± 31 (*n* = 14)	59 ± 17 (*n* = 15)	5,8 ± 1,6 (*n* = 5)	3,5 ± 1,8 (*n* = 5)	0.591 ± 0.035 (*n* = 5)
T2	ST	6 (*n* = 1)	0.022 (*n* = 1)	114 (*n* = 1)	50 (*n* = 1)	2,9 ± 1,6 (*n* = 5)	4,1 ± 0,8 (*n* = 5)	0.584 ± 0.052 (*n* = 5)

Average, standard deviation and sample size (n) were obtained from the full dataset presented in ***Supplementary Tables S1–S3****.*

slopes were not significantly different from the control conditions between T1 and T2 (**Table 1** and **Figure 4**). The *B. nutricula* cells were mainly located in the vicinity of the central capsules, with nearly 8% of the symbionts found in the cytoplasmic extension throughout the gelatinous matrix. During our experiment, the symbiont density varied nearby the central capsule but remained stable for those in the matrix (**Figure 4**).

With respect to photosynthetic parameters, we first measured the oxygen production of entire colonies to globally estimate their overall photosynthesis, then we carried out fluorometric measurements coupled to microscopy to evaluate the photosynthetic efficiency of photosystem II for individual symbiotic cells. Both methods demonstrated that the photosynthetic apparatus was not impacted by neither the stalling nor the thermal stress conditions. Photosynthetic rates remained stable at about 4 μLO_2 mgC^{-1} h^{-1} with no significant changes across all conditions (**Table 1**, **Figure 5a**, and **Supplementary Tables S1, S2**) and the maximal photosystem II quantum yield (F_V/F_M) average was 0.58 (*SD* = 0.04), a nearly optimal value for phytoplanktonic cells (**Table 1**, **Figure 5b**, and **Supplementary Tables S1, S3**). No photoprotective processes of energy dissipation were observed (**Supplementary Tables S1, S3**). Coupling fluorometry analysis to microscopy enabled to measure individual cells photosynthetic capacities. The PAM microscopy analysis thus revealed that at CT-T2 and during the entire heat-stress experiment, the number of observed *B. nutricula* cells per microscopic field decreased, as also suggested by the symbiont density counts. During the experiment, we also observed that the variability of the F_V/F_M increased both within colonies and between colonies, particularly in the stressed treatment where the coefficient of variation significantly increased from T0 to T1 and T2 (**Figure 5b**, **Supplementary Figure S4**, and **Supplementary Tables S1, S4**).

Symbionts Morphological Changes

TEM micrographs were used to monitor ultrastructural changes of the symbiotic *B. nutricula* cells. In control colonies, vacuolar structures containing filamentous particles were observed in cells at T1 (**Figure 6a** and **Supplementary Figure S5**). At T2, these filamentous particles were still present and electron-dense bodies containing membrane-packaged cellular debris appeared within the symbiotic cells (**Figure 6b**) but nuclei as well as chloroplast ultrastructure remained preserved (**Supplementary Figure S6**).

In thermally stressed colonies, filamentous particles were also observed but to a lesser extent. Instead, an important vacuolization around the *B. nutricula* cells, thylakoid disorganization, nucleus dissolution and destabilized organelles structures were observed at 25°C (**Figure 6c**), suggesting autophagic processes. At 28°C, the *B. nutricula* cells from heat-stressed colonies showed marked necrosis patterns with numerous apoptotic bodies and their cellular content appeared completely shrunk, with abundant electron-dense bodies (**Figure 6d**). Inside decaying symbiotic cells, chloroplasts were the only healthy looking organelles, consistent with the maintenance of the photosynthetic capacities observed in the physiological study (**Figure 6** and **Supplementary Figure S6**).

DISCUSSION

Bleaching is commonly described in the phylum Cnidaria as a loss of color originating in the exclusion of the symbiotic dinoflagellates (i.e., genus *Symbiodinium*) from the animal, and/or the degradation of photosynthetic pigments in the chloroplasts of the symbionts (Douglas, 2003). Bleaching has also been shown to occur in the benthic protists Foraminifera (Rhizaria) hosting symbiotic diatoms (Schmidt et al., 2011; Edgar et al., 2013). Here, as symbionts were lightly arranged around the central capsule, the color loss was not detectable to the naked eye, but we observed a decrease of the dinoflagellate symbiont (*B. nutricula*) density in the planktonic species *C. pelagicum* (Collodaria, Retaria) during a heat stress experiment. This study shows that bleaching processes, as initially defined by Kleppel et al. (1989), are not restricted to benthic fauna, but likely constitute a broader stress response in marine organisms harboring photosymbionts. *C. pelagicum* belongs to the most diverse and abundant collodarian clade C7 from the Sphaerozoidae family, which is particularly dominant in coastal

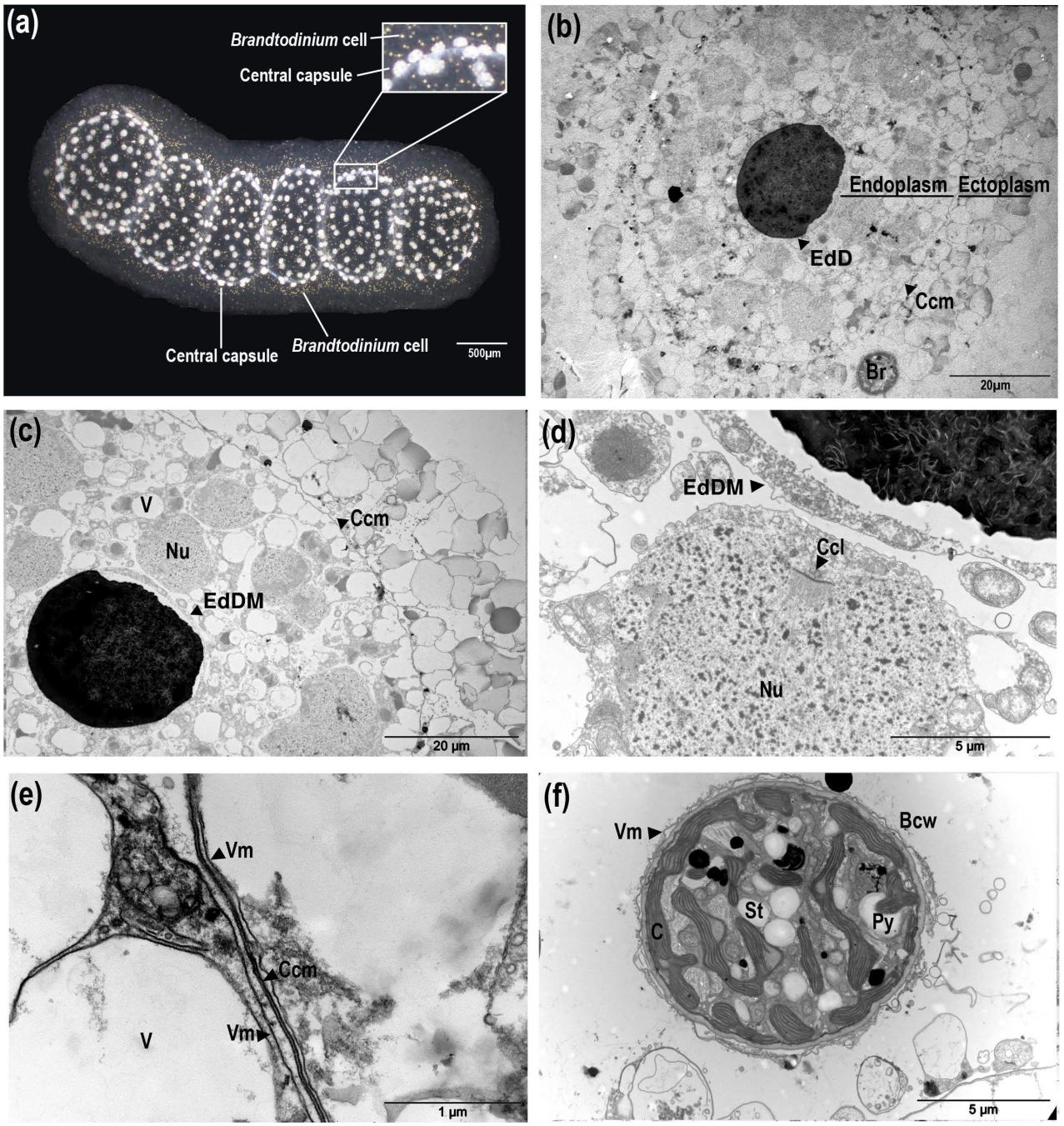

FIGURE 1 | Description of *Collozoum pelagicum* morphology and ultrastructure. *Collozoum pelagicum* colony morphological aspect by binocular observation **(a)**. Observation of the general organization of a central capsule observed by Transmission Electron Microscopy **(b,c)**. Focus on nuclei in the endoplasm of the central capsule **(d)**, membranes at the periphery of the central capsule **(e)** and *in hospite Brandtodinium nutricula* cells **(f)**, observed by electron microscopy. Bcw, *B. nutricula* cell wall; C, Chloroplast; Ccl, cord-like Chromatin; Ccm, Central capsule membrane; EdD, Electron-dense Droplet; EdDM, Electron-dense Droplet Membrane; Nu, Nuclei; Py, Pyrenoid; St, Starch granule; V, Vacuole; Vm, Vacuolar membrane.

biomes and in the western part of the Mediterranean Sea (Biard et al., 2017), stressing out the potential ecological impact of such symbiont loss events in the environment.

Although we cannot exclude that cellular processes involved in the symbiont loss can be radically distinct among different taxa, one might consider that, as described for cnidarians (Weis, 2008), the decrease of symbiont density in *C. pelagicum* could originate in the digestion and/or expulsion of *B. nutricula* cells. Indeed, it has been shown that, under standard conditions, cnidarians continuously expel degraded forms of *Symbiodinium*

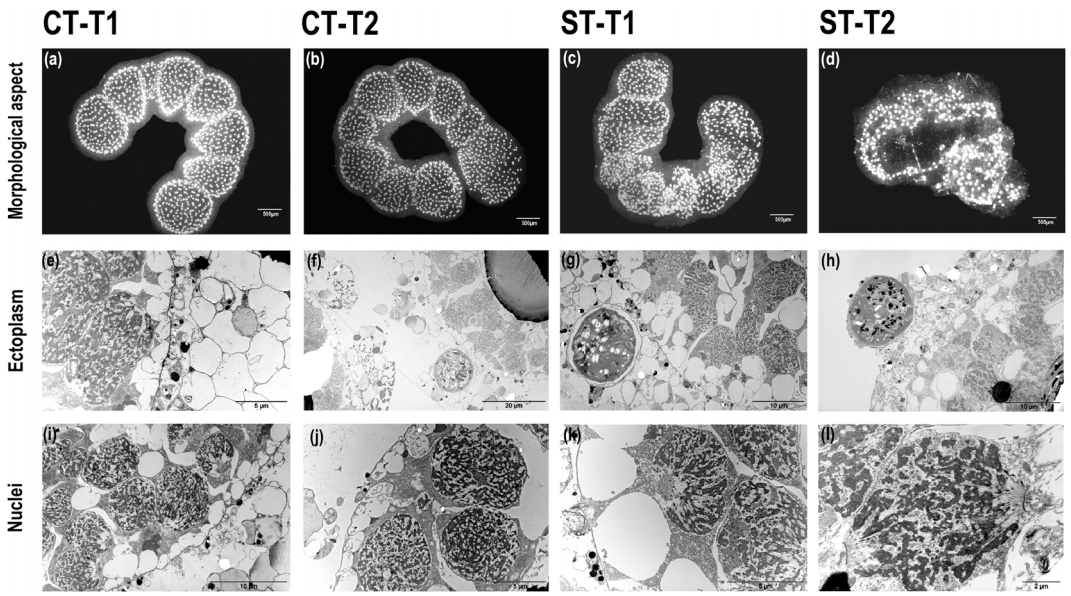

FIGURE 2 | Morphological and ultrastructural changes in control and heat-stressed *Collozoum pelagicum*. Observation of colonies overall morphological aspect at control T1 **(a)** and control T2 **(b)** at 21°C, thermal stress T1 at 25°C **(c)** and thermal stress T2 at 28°C **(d)**. Focus on the ultrastructure of ectoplasm at control T1 **(e)**, control T2 **(f)**, thermal stress T1 **(g),** and thermal stress T2 **(h)**. Focus on the nuclei ultrastructure at control T1 **(i)** and control T2 **(j)**, thermal stress T1 **(k)**, and thermal stress T2 **(l)** arrows.

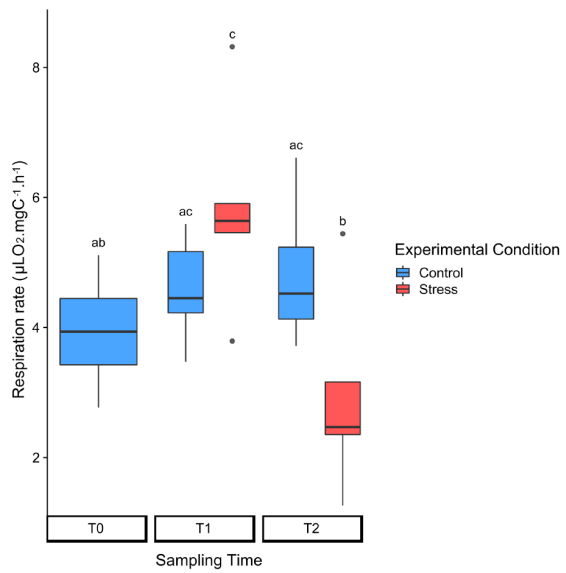

FIGURE 3 | Normalized respiration rates in control (blue) and heat-stressed (red) colonies of *Collozoum pelagicum*. The rates are normalized to the surface area of the colony. Control colonies were maintained at 21°C, while stressed colonies were sampled at 25°C (T1) and 28°C (T2). Pairwise comparison from permutation test between each condition was represented by letters. Statistical supports are described in **Supplementary Tables 1, 4A**.

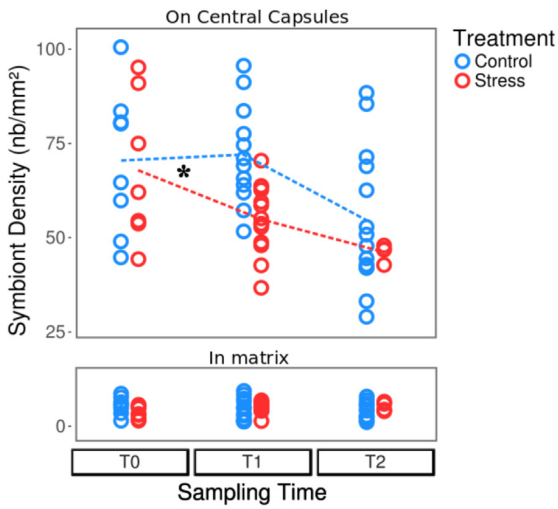

FIGURE 4 | Variations of the symbiont density in control (blue) and heat-stressed colonies (red) of *Collozoum pelagicum*. Control colonies were maintained at 21°C, while stressed colonies were sampled at 21°C (T0), 25°C (T1) and 28°C (T2). The upper and bottom parts represent the density of symbionts attached to central capsules and in the gelatinous matrix, respectively. As indicated by a star, slopes of reaction norms for symbionts from central capsule (represented as dotted lines) were significantly different between T0 and T1 (p-value < 0.025), but not between T1 and T2. Statistical supports are described in **Supplementary Tables 1, 4B,C**.

cells to maintain a healthy population in symbiosis, whereas in stress conditions healthy algal cells are also released in the environment (Ralph et al., 2001; Fujise et al., 2014). In our study, the number of *B. nutricula* cells located at the vicinity of the central capsules decreased, but symbiont density in the gelatinous matrix remained constant. Assuming that expulsion of

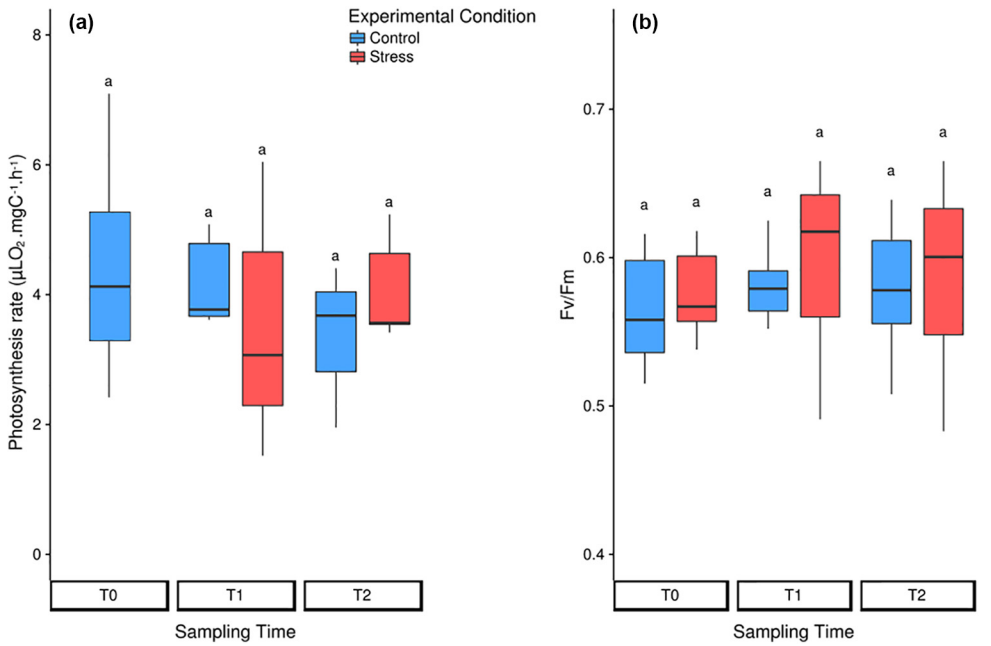

FIGURE 5 | Photosynthetic rates of the symbionts in control (blue) and heat-stressed (red) colonies of *Collozoum pelagicum*. **(a)** Box-plots of photosynthesis rates measured by oxygen production, when normalized by the symbiont surface of the colony. **(b)** Box-plots of PAM-microscopy measurements. Pairwise comparison from permutation test between each condition was represented by letters. Statistical supports are described in **Supplementary Tables 1, 4D,E**.

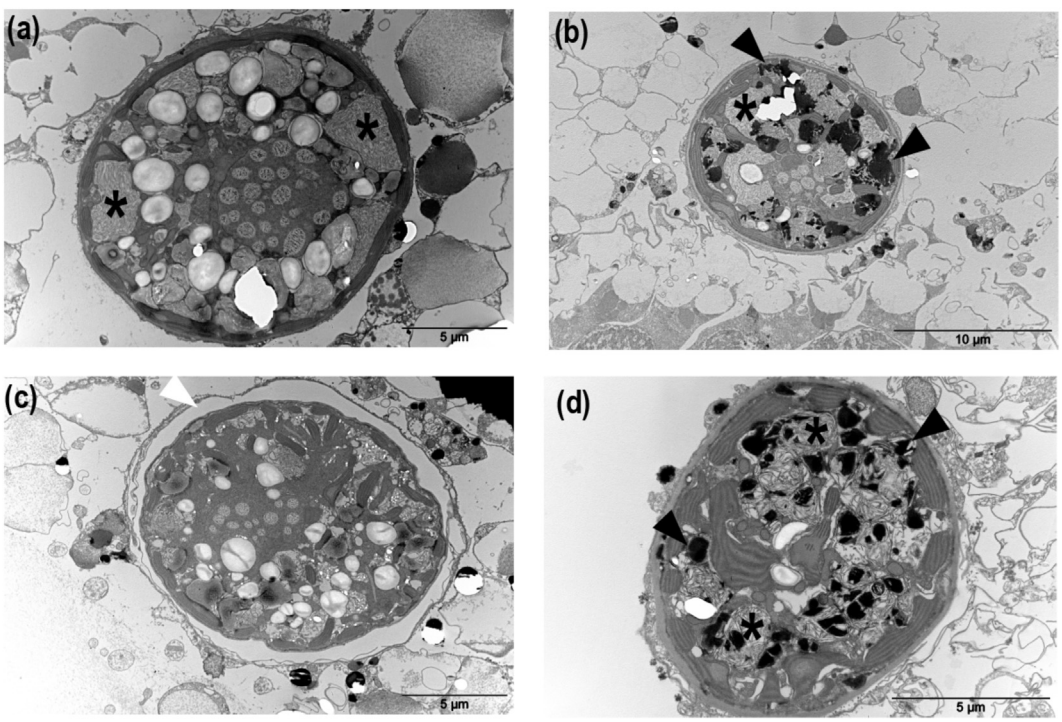

FIGURE 6 | Morphological structures corresponding to the main cellular responses induced in *in hospite B. nutricula* cells in control and heat-stressed colonies of *Collozoum pelagicum*. Transmission electron microscopy of *C. pelagicum* cross section in control T1 **(a)**, control T2 **(b)** at 21°C, and thermal stress T1 at 25°C **(c)** and thermal stress T2 at 28°C **(d)**. Asterisks: filamentous particles, black triangles: apoptotic bodies, white triangles: vacuolar matrix.

B. nutricula cells requires to go through the gelatinous matrix, an increased density would have been expected.

In our study, the respiration rate increase between 21 and 25°C could be related to symbiont digestion. The estimated temperature coefficient Q_{10} for *C. pelagicum* reached the value of 2.66, falling into the Q_{10} range of 2 to 3 estimated for zooplankton (Hernández-León and Ikeda, 2005; Ikeda, 2014). Respiration rate increase as a function of temperature has already been reported in a large panel of zooplankton groups such as Rhizaria, Copepods, Tintinnids (Vidal, 1980; Verity, 1985; Lombard et al., 2005) and could be due to several processes. The global rates of chemical reactions generally increase with temperature (Arrhenius, 1889) and, until enzymatic structure is altered, most biological enzymatic processes require oxygen, so that oxygen demand usually increases with temperature. Also, higher temperatures likely enhance the growth of prokaryotes associated to the host and in turn could contribute to a not negligible part of the holobiont respiration (del Giorgio et al., 1997). Finally, it has also been shown that digestion increases the respiration rate of organisms (Conover, 1978).

Looking at the ultrastructure to characterize the observed bleaching process, all *B. nutricula* cells inside the hosts showed signs of programmed cell death (PCD) mechanisms, such as autophagy (vacuolization) or apoptosis (cell shrinkage, chromatin condensation), suggesting overall cell decay. Apoptosis is triggered by a series of controlled cellular processes involving caspases, which cleave key proteins, cytoskeletal elements and cell adhesion molecules (Dunn et al., 2007). In the autophagic pathway, the target is enveloped in a membrane structure before lysosomal fusion, which initiates digestion by hydrolytic enzymes (Cuervo, 2004). Both apoptosis and autophagy have been observed during cnidarian bleaching and can occur simultaneously (Dunn et al., 2007) or alternatively in response to hyperthermal stress (Richier et al., 2006; Dani et al., 2016). In addition, another process related to symbiotic dinoflagellate autophagy has been reported in cnidarians and is referred to as "symbiophagy," which results in the digestion of the resident dinoflagellates (Downs et al., 2009). TEM observations in *C. pelagicum* suggested that a similar diversity of PCD-like mechanisms would be involved in planktonic symbiosis breakdown. Originally reported in metazoans, PCD-like mechanisms have also been described in phytoplankton in the case of nutrient stress and could occur during viral infections (see review by Bidle, 2015).

Our observations also evidenced the presence of filamentous structures, probably virus-like particles (VLPs), potentially involved in the collapsing of *B. nutricula* cells, whose features appeared similar to the single stranded RNA viruses previously described in *Symbiodinium* cells (Weynberg et al., 2017; Buerger and van Oppen, 2018). These authors indeed proposed that the cnidarian endosymbiont *Symbiodinium* harbors a lysogenic virus within its genome that would induce a lytic infection cycle under stressed conditions. Such lysis of symbiotic dinoflagellates by viruses supports the microbial bleaching hypothesis, which suggests that bleaching could be initiated by the microbial community shift induced by heat-stress (Correa et al., 2016; Thurber et al., 2017). Levin et al. (2017) also described that only thermosensitive *Symbiodinium* showed a marked transcriptional response to viral infection when heat stressed. To our knowledge, only one study has described large icosahedral virus-like particles associated with vacuolar structures in phaeodarians, a taxonomic group close to radiolarians, within the Rhizaria lineage (Gowing, 1993). This study suggests that VLPs could have been acquired by the host through feeding on sinking particles, while in our case, it seems that the viral attack was restricted to the *B. nutricula* cells.

Viral infections in marine algae have been shown to promote ROS activity, triggering subsequent caspase activity and further PCD processes in host cells (Bidle and Vardi, 2011; Bidle, 2015). Nevertheless, as ROS could also be generated by the over-reduction of photosystem I reaction centers (Roberty et al., 2015) during the thermal stress, it was not possible to attribute the cause of the observed PCD directly to the abiotic stress or as a consequence of the pathogen pressure. Weynberg et al. (2017) observed that if nuclear structures were rapidly degraded by virus infection, other organelles like chloroplasts and mitochondria remained almost intact until infectious particles filled the entire cell structure. This is consistent with our observation showing that chloroplasts remained morphologically intact and active, even though other *B. nutricula* organelles were severely damaged. Both oxygen production and fluorometry measurements demonstrated that photosynthesis rates were not altered by heat stress as *B. nutricula* photosynthetic efficiencies remained globally stable. The increased variability of individual photosynthetic efficiencies during heat-stress treatments suggests that healthy *B. nutricula* could compensate for damaged symbionts so as to buffer the holobiont photosynthetic activity.

Based on our observations (e.g., respiration virtually stopped, morphological structure altered), a temperature of 28°C (i.e., T2) likely exceeded the *C. pelagicum* colonies tolerance threshold. The pronounced thermal stress we applied in our experiment aimed at observing and characterizing a marked response of the symbiotic system, likely preventing the potentially existing acclimation period required for the host plastic response. The free-living stage of the microalgal symbionts *B. nutricula* tolerates temperatures up to 29°C when grown in batch culture, displaying relatively high growth rates and photosynthetic efficiency (**Supplementary Figure S7**). *Symbiodinium* physiology was also more affected by heat stress when in symbiosis with corals than when maintained free-living in culture (Buxton et al., 2009). Photosymbiosis induces critical symbiont morphological and physiological changes (i.e., loss of motility) likely leading to a greater sensitivity when host protection is altered and prevent buffering external stressors.

In this study, we show that *C. pelagicum* can exhibit heat-induced bleaching. We unveiled several features of the processes, such as host cells degradation, partial digestion and potential viral infection of the *B. nutricula* cells, while the chloroplast was clearly the last structure to remain active. These results raise questions regarding the underlying cellular processes involved in symbiont loss in *C. pelagicum* and preservation mechanisms of chloroplast activity during *B. nutricula* cell collapsing. Further analysis using complementary approaches like transcriptomics or metabolomics would certainly be helpful to decipher more

precisely the *C. pelagicum* holobiont response to elevated temperatures.

AUTHOR CONTRIBUTIONS

EV, MM-S, CB, EB, TL, and FN performed the experiments. EV performed the PAM fluorometry measurements, image analyses, the statistical treatments and wrote the manuscript. VD contributed to the TEM analyses and manuscript writing. MM-S performed the oxygen measurements. CB performed the sequence analyses. CB, FL, CSi, CSa, and FN commented and contributed to the final version of the manuscript. FN planned and designed the research.

FUNDING

This work benefited from the support of the projects IMPEKAB ANR-15-CE02-0011 and inSIDE ANR-12-JSV7-0009-01 of the French National Research Agency (ANR). This research was supported by the research infrastructure EMBRC-Fr (www.embrc-france.fr). CB received funding from the European Union's Horizon 2020 research and innovation program under the Marie Skłodowska-Curie grant agreement no. 706430 (DYNAMO).

ACKNOWLEDGMENTS

The authors greatly acknowledge the Centre Commun de Microscopie Appliquée (Université Côte d'Azur), especially Sophie Pagnotta who performed the TEM image acquisitions. The authors acknowledge the members of Villefranche-sur-mer oceanological observatory for their help during the experimental work, especially Simon Ramondenc, Guillaume de Liege, David Luquet, Sophie Marro, and Régis Lasbleiz. The manuscript was deposited before peer-review on the pre-print server biorXiv (Villar et al., 2018).

SUPPLEMENTARY MATERIAL

The Supplementary Material for this article can be found online at: https://www.frontiersin.org/articles/10.3389/fmars.2018.00387/full#supplementary-material

REFERENCES

Anderson, O. R. (1976a). Fine structure of a collodarian radiolarian (*Sphaerozoum punctatum* Müller 1858) and cytoplasmic changes during reproduction. *Mar. Micropaleontol.* 1, 287–297. doi: 10.1016/0377-8398(76)90012-8

Anderson, O. R. (1976b). Ultrastructure of a colonial radiolarian *Collozoum inerme* and a cytochemical determination of the role of its zooxanthellae. *Tissue Cell* 8, 195–208. doi: 10.1016/0040-8166(76)90046-X

Anderson, O. R. (1983). *Radiolaria*. New York, NY: Springer New York, doi: 10.1007/978-1-4612-5536-9

Anderson, O. R., Swanberg, N. R., and Bennett, P. (1983). Assimilation of symbiont-derived photosynthates in some solitary and colonial radiolaria. *Mar. Biol.* 77, 265–269. doi: 10.1007/BF00395815

Arrhenius, S. (1889). Über die Reaktionsgeschwindigkeit bei der Inversion von Rohrzucker durch Säuren. *Z. Phys. Chem.* 4, 226–248. doi: 10.1515/zpch-1889-0116

Baghdasarian, G., and Muscatine, L. (2000). Preferential expulsion of dividing algal cells as a mechanism for regulating algal-cnidarian symbiosis. *Biol. Bull.* 199, 278–286. doi: 10.2307/1543184

Baird, A. H., Bhagooli, R., Ralph, P. J., and Takahashi, S. (2009). Coral bleaching: the role of the host. *Trends Ecol. Evol.* 24, 16–20. doi: 10.1016/j.tree.2008.09.005

Biard, T., Bigeard, E., Audic, S., Poulain, J., Gutierrez-Rodriguez, A., Pesant, S., et al. (2017). Biogeography and diversity of Collodaria (Radiolaria) in the global ocean. *ISME J.* 11, 1331–1344. doi: 10.1038/ismej.2017.12

Biard, T., Pillet, L., Decelle, J., Poirier, C., Suzuki, N., and Not, F. (2015). Towards an integrative morpho-molecular classification of the Collodaria (Polycystinea, Radiolaria). *Protist* 166, 374–388. doi: 10.1016/j.protis.2015.05.002

Biard, T., Stemmann, L., Picheral, M., Mayot, N., Vandromme, P., Hauss, H., et al. (2016). In situ imaging reveals the biomass of giant protists in the global ocean. *Nature* 532, 504–507. doi: 10.1038/nature17652

Bidle, K. D. (2015). The molecular ecophysiology of programmed cell death in marine phytoplankton. *Annu. Rev. Mar. Sci.* 7, 341–375. doi: 10.1146/annurev-marine-010213-135014

Bidle, K. D., and Vardi, A. (2011). A chemical arms race at sea mediates algal host–virus interactions. *Curr. Opin. Microbiol.* 14, 449–457. doi: 10.1016/j.mib.2011.07.013

Buerger, P., and van Oppen, M. J. H. (2018). Viruses in corals: hidden drivers of coral bleaching and disease? *Microbiol. Aust.* 2:4. doi: 10.1071/MA18004

Buxton, L., Badger, M., and Ralph, P. (2009). Effects of moderate heat stress and dissolved inorganic carbon concentration on photosynthesis and respiration of *Symbiodinium* Sp. (dinophyceae) in culture and in symbiosis. *J. Phycol.* 45, 357–365. doi: 10.1111/j.1529-8817.2009.00659.x

Cikala, M., Wilm, B., Hobmayer, E., Böttger, A., and David, C. N. (1999). Identification of caspases and apoptosis in the simple metazoan Hydra. *Curr. Biol.* 9, 959–962. doi: 10.1016/S0960-9822(99)80423-0

Conover, R. (1978). "Transformation of organic matter," in *Marine Ecology, Dynamics*, Vol. 4, ed. O. Kinne (New York, NY: Wiley), 221–499.

Correa, A. M. S., Ainsworth, T. D., Rosales, S. M., Thurber, A. R., Butler, C. R., and Vega Thurber, R. L. (2016). Viral outbreak in corals associated with an in situ bleaching event: atypical herpes-like viruses and a new Megavirus infecting *Symbiodinium*. *Front. Microbiol.* 7:127. doi: 10.3389/fmicb.2016.00127

Cuervo, A. M. (2004). Autophagy: many paths to the same end. *Mol. Cell. Biochem.* 263, 55–72. doi: 10.1023/B:MCBI.0000041848.57020.57

Dani, V., Priouzeau, F., Pagnotta, S., Carette, D., Laugier, J.-P., and Sabourault, C. (2016). Thermal and menthol stress induce different cellular events during sea anemone bleaching. *Symbiosis* 69, 175–192. doi: 10.1007/s13199-016-0406-y

Decelle, J., Colin, S., and Foster, R. A. (2015). "Photosymbiosis in marine planktonic protists," in *Marine Protists*, eds S. Ohtsuka, T. Suzaki, T. Horiguchi, N. Suzuki, and F. Not (Tokyo: Springer), 465–500. doi: 10.1007/978-4-431-55130-0_19

del Giorgio, P. A., Cole, J. J., and Cimbleris, A. (1997). Respiration rates in bacteria exceed phytoplankton production in unproductive aquatic systems. *Nature* 385, 148–151. doi: 10.1038/385148a0

Douglas, A. E. (2003). Coral bleaching—how and why? *Mar. Pollut. Bull.* 46, 385–392. doi: 10.1016/S0025-326X(03)00037-7

Downs, C. A., Kramarsky-Winter, E., Martinez, J., Kushmaro, A., Woodley, C. M., Loya, Y., et al. (2009). Symbiophagy as a cellular mechanism for coral bleaching. *Autophagy* 5, 211–216. doi: 10.4161/auto.5.2.7405

Dunn, S. R., Schnitzler, C. E., and Weis, V. M. (2007). Apoptosis and autophagy as mechanisms of dinoflagellate symbiont release during cnidarian bleaching: every which way you lose. *Proc. R. Soc. B Biol. Sci.* 274, 3079–3085. doi: 10.1098/rspb.2007.0711

Edgar, K. M., Bohaty, S., Gibbs, S., Sexton, P., Norris, R., and Wilson, P. (2013). Symbiont 'bleaching'in planktic foraminifera during the Middle Eocene Climatic Optimum. *Geology* 41, 15–18. doi: 10.1130/G33388.1

Fujise, L., Yamashita, H., Suzuki, G., Sasaki, K., Liao, L. M., and Koike, K. (2014). Moderate thermal stress causes active and immediate expulsion of

photosynthetically damaged zooxanthellae (*Symbiodinium*) from corals. *PLoS One* 9:e114321. doi: 10.1371/journal.pone.0114321

Genty, B., Briantais, J.-M., and Baker, N. R. (1989). The relationship between the quantum yield of photosynthetic electron transport and quenching of chlorophyll fluorescence. *Biochim. Biophys. Acta* 990, 87–92. doi: 10.1016/S0304-4165(89)80016-9

Glynn, P. W. (1984). Widespread coral mortality and the 1982–83 el Niño warming event. *Environ. Conserv.* 11, 133–146. doi: 10.1017/S0376892900013825

Gowing, M. M. (1993). Large virus-like particles from vacuoles of phaeodarian radiolarians and from other marine samples. *Mar. Ecol. Prog. Ser.* 101, 33–43. doi: 10.3354/meps101033

Guidi, L., Chaffron, S., Bittner, L., Eveillard, D., Larhlimi, A., Roux, S., et al. (2016). Plankton networks driving carbon export in the oligotrophic ocean. *Nature* 532, 465–470. doi: 10.1038/nature16942

Haeckel, E. (1887). "Report on Radiolaria collected by HMS Challenger during the years 1873-1876. Volume XVIII (Part 1) p. xcix-c," in *The Voyage of HMS Challenger*, eds C. W. Thompson and J. Murray (London: Her Majesty's Stationary Office).

Hernández-León, S., and Ikeda, T. (2005). *Zooplankton Respiration. Respiration in Aquatic Systems*. New York, NY: Oxford University Press, 57–82.

Hoegh-Guldberg, O., Mumby, P. J., Hooten, A. J., Steneck, R. S., Greenfield, P., Gomez, E., et al. (2007). Coral reefs under rapid climate change and ocean acidification. *Science* 318, 1737–1742. doi: 10.1126/science.1152509

Hurlbert, S. H. (1984). Pseudoreplication and the design of ecological field experiments. *Ecol. Monogr.* 54, 187–211. doi: 10.2307/1942661

Ikeda, T. (2014). Respiration and ammonia excretion by marine metazooplankton taxa: synthesis toward a global-bathymetric model. *Mar. Biol.* 161, 2753–2766. doi: 10.1007/s00227-014-2540-5

Katoh, K., Misawa, K., Kuma, K., and Miyata, T. (2002). MAFFT: a novel method for rapid multiple sequence alignment based on fast Fourier transform. *Nucleic Acids Res.* 30, 3059–3066. doi: 10.1093/nar/gkf436

Kleppel, G., Dodge, R. E., and Reese, C. (1989). Changes in pigmentation associated with the bleaching of stony corals. *Limnol. Oceanogr.* 34, 1331–1335. doi: 10.4319/lo.1989.34.7.1331

Lesser, M. P. (2006). Oxidative stress in marine environments: biochemistry and physiological ecology. *Annu. Rev. Physiol.* 68, 253–278. doi: 10.1146/annurev.physiol.68.040104.110001

Lesser, M. P. (2011). "Coral Bleaching: Causes and Mechanisms," in *Coral Reefs: An Ecosystem in Transition*, eds Z. Dubinsky and N. Stambler (Dordrecht: Springer), 405–419. doi: 10.1007/978-94-007-0114-4_23

Levin, R. A., Voolstra, C. R., Weynberg, K. D., and van Oppen, M. J. H. (2017). Evidence for a role of viruses in the thermal sensitivity of coral photosymbionts. *ISME J.* 11, 808–812. doi: 10.1038/ismej.2016.154

Lilley, M. K. S., Thibault-Botha, D., and Lombard, F. (2014). Respiration demands increase significantly with both temperature and mass in the invasive ctenophore *Mnemiopsis leidyi*. *J. Plankton Res.* 36, 831–837. doi: 10.1093/plankt/fbu008

Logan, C. A., Dunne, J. P., Eakin, C. M., and Donner, S. D. (2014). Incorporating adaptive responses into future projections of coral bleaching. *Glob. Chang. Biol.* 20, 125–139. doi: 10.1111/gcb.12390

Lombard, F., Sciandra, A., and Gorsky, G. (2005). Influence of body mass, food concentration, temperature and filtering activity on the oxygen uptake of the appendicularian *Oikopleura dioica*. *Mar. Ecol. Prog. Ser.* 301, 149–158. doi: 10.3354/meps301149

Michaels, A. F., Caron, D. A., Swanberg, N. R., Howse, F. A., and Michaels, C. M. (1995). Planktonic sarcodines (Acantharia, Radiolaria, Foraminifera) in surface waters near Bermuda: abundance, biomass and vertical flux. *J. Plankton Res.* 17, 131–163. doi: 10.1093/plankt/17.1.131

Paxton, C. W., Davy, S. K., and Weis, V. M. (2013). Stress and death of cnidarian host cells play a role in cnidarian bleaching. *J. Exp. Biol.* 216, 2813–2820. doi: 10.1242/jeb.087858

Probert, I., Siano, R., Poirier, C., Decelle, J., Biard, T., Tuji, A., et al. (2014). *Brandtodinium* gen. nov. and B. nutricula comb. Nov. (Dinophyceae), a dinoflagellate commonly found in symbiosis with polycystine radiolarians. *J. Phycol.* 50, 388–399. doi: 10.1111/jpy.12174

R Core Team (2013). *R: A Language and Environment for Statistical Computing*. Vienna: R Foundation for Statistical Computing.

Ralph, P. J., Gademann, R., and Larkum, A. W. (2001). Zooxanthellae expelled from bleached corals at 33°C are photosynthetically competent. *Mar. Ecol. Prog. Ser.* 220, 163–168. doi: 10.3354/meps220163

Rasband, W. (1997). *ImageJ*. Bethesda, MD: US National Institutes of Health.

Richier, S., Sabourault, C., Courtiade, J., Zucchini, N., Allemand, D., and Furla, P. (2006). Oxidative stress and apoptotic events during thermal stress in the symbiotic sea anemone, *Anemonia viridis*. *FEBS J.* 273, 4186–4198. doi: 10.1111/j.1742-4658.2006.05414.x

Roberty, S., Fransolet, D., Cardol, P., Plumier, J.-C., and Franck, F. (2015). Imbalance between oxygen photoreduction and antioxidant capacities in Symbiodinium cells exposed to combined heat and high light stress. *Coral Reefs* 34, 1063–1073. doi: 10.1007/s00338-015-1328-5

Schmidt, C., Heinz, P., Kucera, M., and Uthicke, S. (2011). Temperature-induced stress leads to bleaching in larger benthic foraminifera hosting endosymbiotic diatoms. *Limnol. Oceanogr.* 56, 1587–1602. doi: 10.4319/lo.2011.56.5.1587

Stamatakis, A. (2014). RAxML version 8: a tool for phylogenetic analysis and post-analysis of large phylogenies. *Bioinformatics* 30, 1312–1313. doi: 10.1093/bioinformatics/btu033

Swanberg, N. R. (1983). The trophic role of colonial Radiolaria in oligotrophic oceanic environments1,2. *Limnol. Oceanogr.* 28, 655–666. doi: 10.4319/lo.1983.28.4.0655

Thurber, R. V., Payet, J. P., Thurber, A. R., and Correa, A. M. S. (2017). Virus–host interactions and their roles in coral reef health and disease. *Nat. Rev. Microbiol.* 15, 205–216. doi: 10.1038/nrmicro.2016.176

Verity, P. G. (1985). Grazing, respiration, excretion, and growth rates of tintinnids. *Limnol. Oceanogr.* 30, 1268–1282. doi: 10.4319/lo.1985.30.6.1268

Vidal, J. (1980). Physioecology of zooplankton. IV. Effects of phytoplankton concentration, temperature, and body size on the net production efficiency of *Calanus pacificus*. *Mar. Biol.* 56, 203–211. doi: 10.1007/BF00645344

Villar, E., Dani, V., Bigeard, E., Linhart, T., Mendez-Sandin, M., Bachy, C., et al. (2018). Chloroplasts of symbiotic microalgae remain active during bleaching induced by thermal stress in Collodaria (Radiolaria). *bioRxiv* [Preprint]. doi: 10.1101/263053

Weis, V. M. (2008). Cellular mechanisms of Cnidarian bleaching: stress causes the collapse of symbiosis. *J. Exp. Biol.* 211, 3059–3066. doi: 10.1242/jeb.009597

Weynberg, K. D., Neave, M., Clode, P. L., Voolstra, C. R., Brownlee, C., Laffy, P., et al. (2017). Prevalent and persistent viral infection in cultures of the coral algal endosymbiont Symbiodinium. *Coral Reefs* 36, 773–784. doi: 10.1007/s00338-017-1568-7

Conflict of Interest Statement: The authors declare that the research was conducted in the absence of any commercial or financial relationships that could be construed as a potential conflict of interest.